Project Title:
Using remote sensing to map *Arundo donax* populations in Native Fish Conservation Areas throughout Texas to better understand causal factors of invasion and set management priorities.

Grant #:
CA-0002195

Project Personnel:

Dr. Jason Martina, Principal Investigator
Department of Biology
Texas State University
San Marcos, TX 78666
jpmartina@txstate.edu
512-245-0565

Dr. Jennifer Jensen, Co-Principal Investigator
Department of Geography and Environmental Studies
Texas State University
San Marcos, TX 78666
jjensen@txstate.edu
512-245-1724

Jenna DeMent, MS Student
Department of Biology
Texas State University
San Marcos, TX 78666
Mtl77@txstate.edu

TPWD Coordinator:

Monica McGarrity, TPWD Project Coordinator
Senior Scientist for Aquatic Invasive Species
Inland Fisheries Division – Habitat Conservation Branch
Texas Parks and Wildlife Department
4200 Smith School Rd., Austin, TX 78744
Cell: 512-552-3465

Executive Summary:

The invasive grass *Arundo donax* (hereafter *Arundo*) is a large stature nuisance plant species that is currently spreading throughout Texas, mainly around waterways. Where it establishes it can pose a significant threat to the health of riversides and stream channels by out-competing native vegetation, increasing erosion, altering flood control potential and fire regimes, and reducing wildlife habitat quality. There is a substantial need in Texas to map locations of successful *Arundo* invasion, especially in NFCAs, to better establish management and restoration priorities. There are currently large geographic areas within NFCAs that are not monitored on the ground for the presence of *Arundo* due to the time investment needed for such a large undertaking. Here we attempted a statewide detection and inventory project of current and past *Arundo* invasion in Native Fish Conservation Areas (NFCAs). We mapped areas of established populations and detect rates of expansion using remote sensing techniques. Our project developed methods that will allow for detection through remote sensing products on large geographic scales.

Our project had three main objectives:

Objective 1 – Inventory and document *Arundo* spectral biosignatures, establish statistical linkages between multispectral sUAS and Sentinel-2 imagery, develop a model to identify *Arundo* using satellite imagery, and map Arundo in two NFCAs of known occurrence.

- Initial field-based accuracy assessments yielded an overall classification accuracy of 71% and a kappa value of 0.46 within training NFCAs of the Guadalupe and San Antonio Rivers (GUAD) and the Southern Edwards Plateau (SEP).
- The overall accuracy indicates that 71% of pixels within this training area were correctly classified as *Arundo* or non-*Arundo* vegetation. The Kappa coefficient of agreement value of 0.46 indicates that the classification has moderate agreement compared to chance alone.
- *Arundo* was detected most frequently along urban or suburban areas with intersecting river systems, while less developed areas had fewer classified pixels of *Arundo*.
- Future iterations of the predictive mapping methodology may be improved by the incorporation of more fine spatial resolution imagery and the consideration of regionally based training imagery.

Objective 2 - The goal was to use Sentinel-2 remote sensing data to map *Arundo* presence and proportion in all NFCAs identified as having potential for infestations and determine rates of expansion from 2015 - present.

- Metrics of accuracy validation for individual or paired NFCAs other than the SEP and GUAD were suboptimal despite several iterations of CART rule adjustments. We attribute this to high phenotypic variability of *Arundo* and the use of relatively coarse imagery resolution at 10 x 10 m pixels. Future remote sensing-based projects looking to differentiate vegetation species based on spectral responses would benefit from purchasing of higher resolution imagery.
- SEP expansion from 2015 – 2018 had a 0.028% gain per year for *Arundo* cover, though this increased between 2018 – 2021 to a 0.54% yearly gain. As this area was exiting the drought of 2015, this gain was anticipated as *Arundo* is highly reliant on freshwater availability.

- The overall expansion rate of 0.284% per year within SEP indicates class coverage of *Arundo* increasing.
- GUAD expansion from 2015 – 2018, on the other hand, experienced a 0.0000067% loss per year of *Arundo* cover, shifting to a gain of 0.00033% per year between 2018 -2021. This loss of *Arundo* is likely from TPWD management efforts rather than any environmental factors or decreasing *Arundo* fitness.
- SEP patch numbers increase quickly and consistently, while GUAD patch numbers decreased sharply between 2015 and 2018.
- GUAD average patch area showed an initial decrease followed by a partial regrowth. This pattern suggests a die back of *Arundo* across GUAD that was followed by additional growth in the following years.

Objective 3 –Establish relationship between landscape features and *Arundo* dominance and spread and identify areas of high management priority.

- Due to challenges in objectives 1 and 2 this objective was not able to be completed. In addition, the poor accuracy of the majority of the eastern and western NFCAs made this analysis non-productive as any landscape feature associations found would likely not be reliable.

This project provides framework for continued remote sensing-based detection methods of a conspicuous invasive species of significant habitat management concern within Texas NFCAs. Though there were issues with model accuracy, this is the first attempt at creating fully remote sensing-based inventory of *Arundo* along with evaluation of expansion rates within Central Texas NFCAs. While we addressed complications encountered and sources of expected error in the report, this project does supplement knowledge gaps regarding expansion characteristics of *Arundo* within Central Texas. It is our hope that the methods and recommendations included in this report will be incorporated into TPWD's ongoing *Arundo* management efforts within and beyond the SEP and GUAD NFCAs. Continued mapping of the *Arundo* using higher resolution imagery than used in this project will provide agencies with a more complete picture of how widespread invasions have become within NFCAs, along with how the invasion has spread in this 7-year time span. A more robust analysis may stem from this methodology for a more complete consideration of influential landscape features contributing to past and future infestations.

Introduction:

Arundo donax (hereafter *Arundo*) is a perennial nonindigenous grass that has been introduced and established in the southern part of the continental United States as well as Hawaii, Puerto Rico, and the Virgin Islands (USDA 2020). *Arundo* is hypothesized to have originated in Asia and diffused through the Mediterranean to North America in the early 1800s (Ahmad et al. 2008, Hardion et al. 2014). Genetic analysis of individuals in North America revealed that all sampled *Arundo* were genetically identical with the exception of one sample found in Texas that exhibited a single mutation (Ahmad et al. 2008). There is evidence that *Arundo* invasions in northern Mexico and southwestern United States are from a single lineage (Tarin et al. 2013). Further investigation into the reproductive mechanisms of *Arundo* shows that the North American invader is sterile and incapable of reproducing via seed. Post-meiotic mutations of the ovule and pollen were found to render the plant infertile (Mariani et al. 2010). The spread of *Arundo* through North America can be attributed to asexual vegetative reproduction via layering, rhizomes, and fragmentation (Decruyenaere and Holt 2001, Boland 2006, Ahmad et al. 2008). The current hypothesis explaining the spread of *Arundo* is that rhizome and stem fragments are dispersed through flood events that carry propagules downstream, allowing them to establish in areas that have been disturbed (Bell 1997, Mariani et al. 2010). Alternative hypotheses propose that flooding may not be the primary driver of *Arundo* spread attributing the expansion of the species to bulldozing and layering (Boland 2006, Boland 2008).

The fast growth of *Arundo* along with its lack of natural enemies has made the species an aggressive and successful invader in the southern United States. *Arundo* can grow up to 10 meters tall, forming dense monotypic stands that are associated with lower species richness in stream banks and floodplains and has been linked to decreased streamflow in the Nueces River (Cushman and Gaffney 2010, Jain et al. 2015). The height of this species confers a competitive advantage over shorter statured native species. The species is typically found along disturbed stream beds, lakes, and other wet areas and can grow 30-70 cm per week under ideal conditions (Perdue 1958, Bell 1997). The fast growth rate and height of *Arundo* allows it to displace native species, especially under high nitrogen and ideal soil moisture regimes.

The success of *Arundo* poses a problem to native arthropod communities by changing the vegetation structure of native habitats. The exotic cattle tick *Rhipicephalus* (*Boophilus*) spp. was shown to be more successful under the abiotic and biotic conditions created by stands of *Arundo* (Racelis et al. 2012). Invasion by large statured invasive grasses, such as *Arundo*, are known to alter the structure of vegetation and reduce arthropod diversity, which in turn leads to decreased avian diversity (Herrera and Dudley 2003, Kisner 2004). There is a lack of evidence that *Arundo* acts as a significant food source or habitat for native wildlife (Bell 1997).

Research on biological control of *Arundo* has been conducted using *Rhizaspidiotus donacis,* an armored scale, and *Tetramesa romana,* a stem-galling wasp, frequently found within the native range of *Arundo* (Moore et al. 2010) as well as being present in Texas. These biological control agents have thus far had negative impacts on *Arundo* populations in an experimental setting, decreasing biomass by 22-32% (Goolsby et al. 2016). Even with biological control and species management programs in place *Arundo* continues to invade susceptible riparian ecosystems throughout Texas.

Factors influencing the success of Arundo

Past studies have examined some of the biotic and abiotic factors that can influence *Arundo*'s successful establishment and expansion. As mentioned above, while current hypotheses explaining the spread of *Arundo* focus on the dispersal of propagules downstream by flood events (Bell 1997, Mariani et al. 2010), it is very likely that a suite of factors influence the successful colonization and spread of *Arundo.*

Arundo can be found in a wide range of soils from dense clays to loose sand and is tolerant of high salinity conditions (Perdue 1958, DiMola et al. 2018). Though capable of withstanding extreme drought and excessive soil moisture, *Arundo* seems to be most successful in areas with well-drained soil and ample moisture (Perdue 1958). The growth of *Arundo* has been found to be closely correlated to soil moisture (Quinn et al. 2008, Nackley et al. 2014). In a study performed by Quinn (2008), it was found that *Arundo* exhibited a positive response to soil moisture and disturbance. In a greenhouse study of the abiotic factors associated with *Arundo* performance (e.g., growth, photosynthetic rate, biomass production), Herod and Martina (2023) found that soil moisture and light strongly interacted to increase growth in high light and soil moisture conditions. As is the case with many competitive species, *Arundo* thrives in disturbed areas and is tolerant of conditions that may be detrimental to native species.

Though able to subsist in infertile conditions, *Arundo* appears to perform the best in high nitrogen conditions (Perdue 1958). The plant seems to favor nitrogen delivered as NH_4^+ or NH_4^+ NO_3^-, as opposed to solely NO_3^- (Tho et al. 2017). Under low nitrogen regimes, *Arundo* tends to exhibit greater distance between buds on the rhizome and more extensive underground structures (Perdue 1958). As is the case with many invasive species, *Arundo* shows higher biomass and spread in response to increased nitrogen (Quinn et al. 2007, Nackley et al. 2017, Tho et al. 2017). Studies indicate that fast-growing invasive species, such as *Arundo*, may gain a competitive advantage over native species when N is increased. It is suggested that this may lead to a positive feedback loop in which invasive species are able to, through faster growth and larger size, outcompete native species for resources, mainly light (Mangla et al. 2011). This idea is supported by the success of many large statured wetland species grown in high nitrogen conditions, such as *Phragmites australis* (Martina et al. 2016), *Typha domingensis,* and *Phalaris arundinacea* (Green and Galatowitsch 2001, Minchinton and Bertness 2003, Escutia-Lara et al. 2007, Martina and von Ende 2012). However, Herod and Martina (2023) found that while high N and P did significantly influence internal resource allocation of *Arundo*, their effects on growth and biomass production were dwarfed by the significant effects of soil moisture and light.

Though the presence of established native communities and competitors has not been studied at length in *Arundo,* there is evidence that *Arundo* is mostly unaffected by native community composition or the presence of a competitor. In a study conducted by Quinn (2007), *Arundo* biomass was not significantly affected by competition with *Schoenoplectus pungens* though tiller production was slightly reduced. The results of this study indicate that nitrogen enrichment may be able to make up for the negative effects of competition in *Arundo* establishment. A separate study revealed that the establishment success of *Arundo* was unaffected by the composition of native communities consisting of *Schoenoplectus pungens, Baccharis salicifolia,* and *Salix gooddingii*. When grown with other weedy species, *Arundo* initially exhibited lower values for performance-related traits; however, *Arundo* appeared to become more competitive during the second growing season as it established (Curt et al. 2017).

Key information gaps

Given the characteristics of *Arundo* growth combined with its lack of natural enemies in North America and extreme tolerance to disturbance, the species has become a significant threat to riparian habitats throughout southern United States, and especially in Texas. Management efforts using chemical and mechanical methods have all been used in the field in an effort to control *Arundo,* while biocontrol has been researched (Bell 1997, Moore et al. 2010). Management of *Arundo* can take multiple years, and the success of any given method of control is largely dependent upon knowing the location of infestations, continued treatment, and the characteristics of the ecosystem being managed.

The Texas Native Fish Conservation Areas Network is an integrated and holistic approach to the conservation of freshwater systems (springs, creeks, rivers, and watersheds) throughout Texas. The main function of the NFCAs is the protection of the over 190 species of native freshwater fishes found in Texas, with almost 50% considered imperiled. The threat to these freshwater systems mainly comes from anthropogenically-induced disturbance, including the spread of many invasive species, including *Arundo*, which can greatly alter the river/stream ecosystem in a similar way to *Phragmites australis*, a comparable species known to negatively influence native fish habitats (Lambert et al 2010, Able and Ragan 2003). There is a gap in our knowledge of where successful populations of *Arundo* are located throughout the NFCAs, how fast *Arundo* populations spread, and what landscape factors (such as proximity to human infrastructure or other *Arundo* populations) influence the success and management of this species.

Our research project addressed these key information gaps by mapping areas of established populations and detecting rates of expansion using remote sensing techniques. This project focused on the following TPWD priority aquatic invasive species research topics: 1) Identification of geographic areas and/or habitats most at risk of invasion and impacts in Texas and 2) Determine the geographic distribution and dispersal of aquatic invasive species in Texas. In addition, by analyzing the rate of invasion through time and connecting expansion rates with causal landscape features, we addressed a third priority topic "Ecology and population dynamics of problematic aquatic invasive species in Texas, with a focus on factors affecting invasion success or management implications".

Project Objectives:

Objective 1 – Inventory and document *Arundo* spectral biosignatures, establish statistical linkages between multispectral sUAS and Sentinel-2 imagery, develop a model to identify *Arundo* using satellite imagery, and map *Arundo* in two NFCAs of known occurrence.

Objective 2 - Use Sentinel-2 remote sensing data to map *Arundo* presence and proportion in all NFCAs identified as having potential for infestations and determine rates of expansion from 2015 - present.

Objective 3 – Establish relationship between landscape features and *Arundo* dominance and spread and identify areas of high management priority.

Methods:

A current challenge with identification of *Arundo* throughout Texas is that existing methods rely on aerial surveys and boots-on-the ground mapping to build and update existing inventories; however, this process is expensive and time consuming. Vegetation, like all surface materials, has a specific electromagnetic (EM) response to incoming solar radiation. For vegetation, the relationship between chlorophyll absorption of red wavelengths and strong reflectance of near-infrared wavelengths within the intracellular air spaces of plants provides a key indicator of plant presence growth, photosynthetic capacity, vigor, etc. Additionally, these surface-energy interactions in the red and near-infrared region of the EM spectrum facilitate mapping of individual species as well as vegetation community composition as different plant species have different spectral responses. A key wavelength region of interest in vegetation studies is termed the red-edge. The red-edge is the region in the EM spectrum where a sharp increase in NIR leaf reflectance occurs and is considered a spectroscopic biosignature of vegetation. Many aerial and satellite sensors can be used to approximate the magnitude of NIR leaf reflectance, but few sensors actually measure red-edge reflectance.

Although small unmanned aerial systems (sUAS) have been increasingly used to map vegetation, the sensors often record basic red, green, and blue (RGB) wavelengths and are not radiometrically calibrated such that the spectral response recorded by the sensors can be transferrable to other sites or different collection days. The sUAS used for this project has six radiometrically calibrated individual sensors; one for RBG imaging and five monochromatic sensors for multispectral imaging. Of keen importance are the red, near-infrared, and red-edge sensors on-board the multispectral system and that they correspond to the red, near-infrared, and red-edge regions also measured by the Sentinel-2 satellite system. Sentinel-2 is a two-constellation satellite operated by the European Space Agency to acquire repeat imagery every 2-5 days at 10-, 20-, and 60-meter spatial resolutions (ground sample distances). We used the multispectral sUAS (DJI Phantom 4 Multispectral) to scale the spectral response of *Arundo* to Sentinel-2 imagery for the purposes of identifying the spectral relationships between the two sensors and then mapping *Arundo* in un-inventoried areas using classification and regression tree predictive models.

OBJECTIVE 1: Creation of 2022 *Arundo* Inventory

Field Collections

To create the 2022 predictive model, we first gathered high-resolution spectral imagery of known *Arundo* populations. Initial imagery collection of *Arundo* training points was performed with a DJI Phantom 4 sUAS equipped with a multispectral camera suited for capturing spectral responses lending to computation of several Spectral Vegetation Indices (SVIs). Flight locations had a tiered, targeted approach with the following requirements: (1) being within one of the targeted training NFCAs, (2) having known *Arundo* infestations, and (3) being accessible for safe sUAS launch, flight, and landing. Based on these criteria, we selected the Guadalupe and San Antonio Rivers (GUAD), as well as the Southern Edwards Plateau (SEP) NFCAs for training data collection (Figure 1). Focal rivers included the Guadalupe, Blanco, and Medina Rivers where TPWD data layers from the *Arundo* management oriented Healthy Creeks Initiative had documented *Arundo* locations via aerial survey (Figure 1).

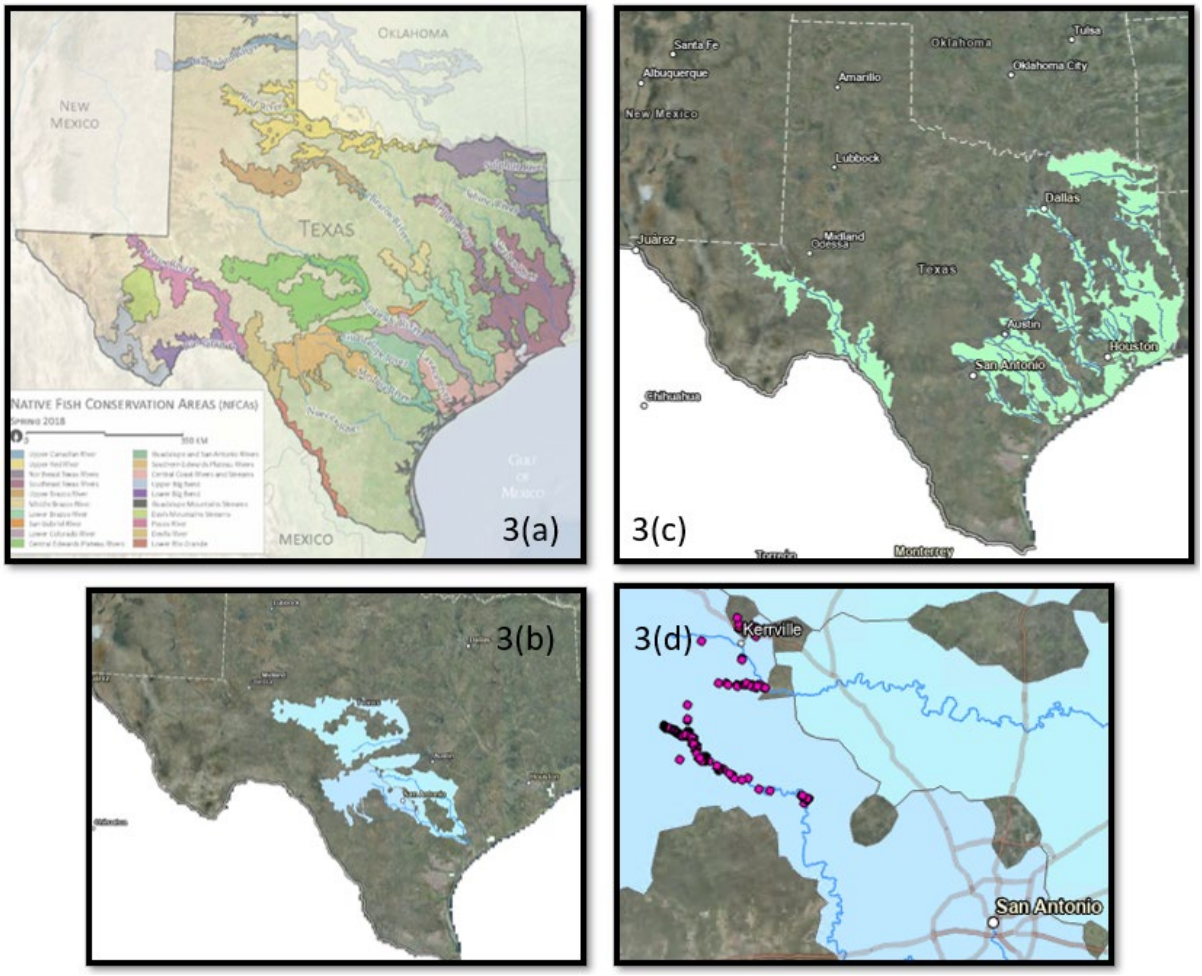

Figure 1: Map examples of the study area. 3(a) Map of Native Fish Conservation Areas of Texas, sourced from the Native Fish Conservation Network Conservation Planning Map. 3*(b)* Training NFCAs used for initial sUAS imagery collection and model training. Guadalupe & San Antonio Rivers and Southern Edwards Plateau NFCAs were selected based on presence of known *Arundo* infestations. 3(c) Stage 2 NFCAs where developed model was applied for *Arundo* classification based on Sentinel-2 imagery. 3(d) Known *Arundo* populations (point data) selected for initial sUAS imagery collection within Training NFCAs. Data provided by TPWD's Healthy Creek Initiative 2019 Survey.

Safety of launch locations were individually evaluated with consideration of public access. When possible, flights were performed between 10:00 am and 11:00 am to best coincide with Sentinel-2 overpass. The goal altitude for flights was maintained at 150 m which yielded an average spatial resolution of 0.083 m and swath width of 173 m. The sUAS imagery collections were targeted for the summer season, when *Arundo* is flushed green and characteristic inflorescences have emerged. These characteristics assisted in visual delineation of *Arundo* canopy cover within the imagery (Figure 2).

During each flight, the sUAS captured images of reflectance targets so that the data can be calibrated to known surface reflectance. Calibrated images were processed in Agisoft Metashape to create fully georeferenced digital orthomosaics of each mission. *In-situ* measurements of *Arundo* were overlain on the orthomosaics to determine *Arundo* presence and to guide image interpretation efforts to identify additional stands not accessible by foot. Stands were manually digitized on-screen

and the spectral responses in the red, NIR, and red-edge wavelength regions were recorded for analysis.

Figure 2: Examples of an *Arundo* stand along the Blanco River in San Marcos, Texas. Inflorescences and unique shadow casting simplified visual identification, though mixed pixels may complicate a clear species-specific spectral response isolation.

A total of 31 individual sUAS flights were performed (Table 1). Of these, 20 were referenced for the digital delineation of *Arundo* canopy footprints from June and July 2022 collections. The 11 flights not used were excluded due to poor flight conditions (e.g., high winds or inappropriate sun angles) decreasing the reliability of the imagery. These flights were re-flown for improved imagery acquisition. In areas flown more than once, the cleanest sUAS data was retained. November 2021 sUAS data along portions of the Blanco River north of San Marcos, Texas were used as preliminary training flights to assure correct sUAS operation and post-processing. Agisoft Metashape was used for mosaicking individual = sUAS images into a larger, high-spatial accuracy output. Following this, the mosaicked image was imported to ArcGIS Pro for digital delineation of visually identifiable *Arundo* stands (Figure 3).

Table 1: Summary of completed flights, with general location, dates, and river corridor distance spanned by imagery collection (km). *November 2021 preliminary training flights.

River	Flights Total	Flights Used	Approx Distance (km)	Dates	Nearest City
Blanco	15	8	5.44	July 2022 & November 2021*	San Marcos
Medina	11	7	4.89	Jun-22	Medina & Bandera
Guadalupe	5	5	3.09	Jun-22	Kerrville

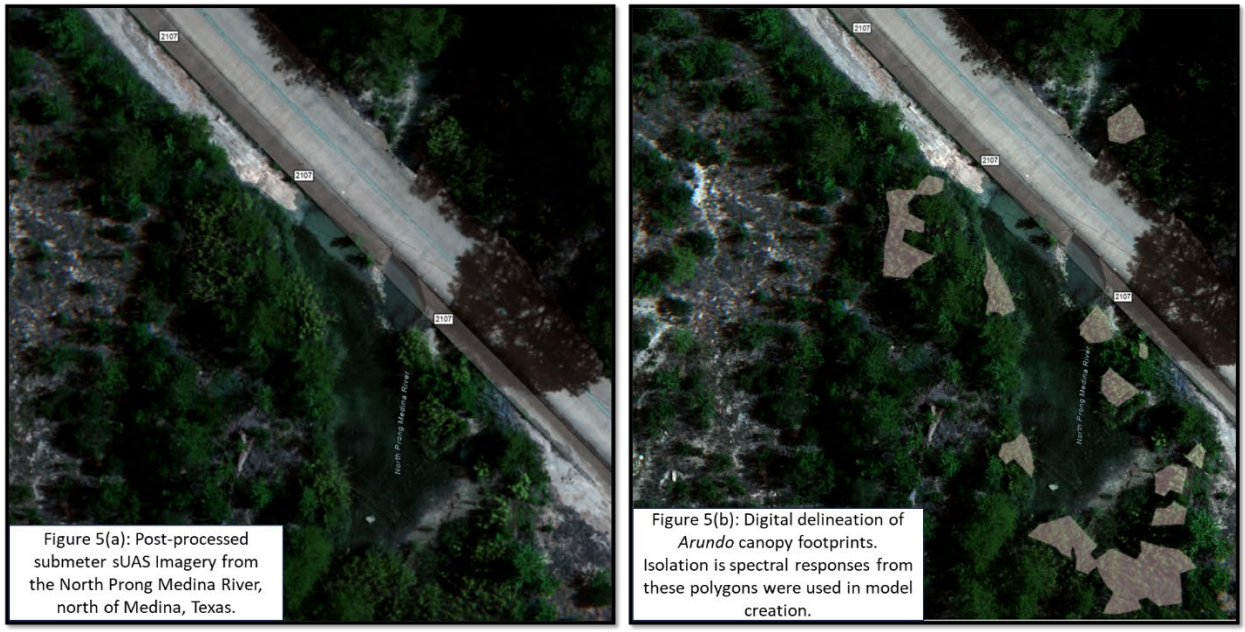

Figure 3: Post-processed sUAS imagery and *Arundo* delineation example. Snapshot of a June flight from the North Prong tributary of the Medina River.

While flights were performed remotely with few restrictions, more complete ground-truthing community surveys of *Arundo* stands were often restricted due to property access denial. With 93% of Texas' land area being privately owned, this was an anticipated complication (Texas Parks and Wildlife Department, n.d.). When *Arundo* stands were on publicly accessible land or express landowner permission was granted, a Trimble Geo7XH GPS unit was used to document the canopy footprint of the stands. Complete community data was collected from 12 *Arundo* stands (Table S1). These field data were later referenced during model development to verify *Arundo* and non-*Arundo* classified pixels. When access was denied by landowners or deemed unsafe, the submeter sUAS imagery processed in Agisoft Metashape was instead referenced to delineate *Arundo* canopy footprints. While not incorporated in our analysis due to poor sample size (attributed with access restrictions), this species composition data was useful in retroactively validating pixel classifications of *Arundo* and non-*Arundo* coverage within the model.

Imagery Preparation & Comparison to Acquired Sentinel-2 Imagery

Sentinel-2 imagery gathered from dates on or near the date of sUAS flights over identified *Arundo* populations was obtained and processed to isolate surface reflectance products. Per objective 1 methods, these were late summer dates generally falling around August and September. Sentinel-2 imagery was acquired from the Copernicus Access Hub as open-source data maintained by the European Space Agency (ESA). We emphasized acquisition of Sentinel-2 processing Level-2A imagery as these come with surface reflectance values calculated. When Level-2A was unavailable, Level-1C products were instead acquired. However, Level-1C is only processed to top-of-atmosphere (TOA) reflectance. Since TOA products have not yet been corrected for atmospheric constituents and variability (e.g., gases, aerosol presence), additional processing was required for these downloads. ESA's SNAP Desktop was used with the Sen2Cor processor to address the required atmospheric corrections and create a more suitable Level-2A product with surface reflectance values.

The Sentinel-2 satellite is equipped with a Multispectral Imager calibrated to detect 13 spectral bands ranging from 10 – 60 m pixel size (Table 2) (European Space Agency, 2015). Though *Arundo* can form hectares of monocultures (Boland, 2006; Mariani et al., 2010), this is uncommon in our study region. For this reason, any bands selected for investigation were resampled to 10 m using nearest neighbor statistics in ArcGIS Pro. This higher spatial resolution should improve the predictive capabilities of our mapped inventory. Bands 4-8 and band 8a were initially isolated for investigation as these bands are well documented in the calculation of SVIs capable of identifying functional groups or specific species (Vogelmann et al., 1993).

Table 2: Sentinel-2 Spectral Bands. Bands 4-8 and 8a were selected for investigation. Use of these spectral ranges for calculations of SVIs are well documented (European Space Agency, 2015; Vogelmann et al., 1993).

Band	Resolution	Central Wavelength	Description
B1	60 m	443 nm	Ultra blue (Coastal and Aerosol)
B2	10 m	490 nm	Blue
B3	10 m	560 nm	Green
B4	10 m	665 nm	Red
B5	20 m	705 nm	Visible and Near Infrared (VNIR)
B6	20 m	740 nm	Visible and Near Infrared (VNIR)
B7	20 m	783 nm	Visible and Near Infrared (VNIR)
B8	10 m	842 nm	Visible and Near Infrared (VNIR)
B8a	20 m	865 nm	Visible and Near Infrared (VNIR)
B9	60 m	940 nm	Short Wave Infrared (SWIR)
B10	60 m	1375 nm	Short Wave Infrared (SWIR)
B11	20 m	1610 nm	Short Wave Infrared (SWIR)
B12	20 m	2190 nm	Short Wave Infrared (SWIR)

With imagery acquired, surface reflectance calculated, and bands isolated, imagery underwent additional preparatory steps. Due to the significant computing demands that come with broad scale imagery classification and model application, we opted to emphasize mainstem river corridors within the NFCAs. Application, in this sense, means instructing this model to classify individual 10 m pixels of Sentinel-2 imagery across our study area as either "*Arundo*" or "non-*Arundo*". In ArcGIS Pro, individual spectral layers were restricted to 200 m buffers of the focal rivers to streamline processing and reduce expected errors anticipated from inclusion of non-riparian species. All processing layers and bands were projected into the World Geodetic System 1984/Universal Transverse Mercator 14N for spatially relevant computation.

Using known locations of *Arundo* digitized during sUAS imagery acquisition, Sentinel-2A clipped bands were stacked and isolated for investigation. Red, NIR, and red-edge responses were extracted for the final model approach. SVIs of the training NFCAs were calculated from these bands and included the Vegetation Red-Edge Index (Vogelmann et al., 1993), Red-Edge

Normalized Difference Vegetation Index (Gitelson & Merzlyak, 1994), and more common indices including the Normalized Difference Vegetation Index (Rouse et al., 1974).

Modeling Methods & Accuracy Assessment

The mapping model algorithm was developed using a Classification and Regression Tree (CART) analysis in JMP Pro to determine presence and absence of *Arundo* in Sentinel-2's 10 m imagery. CART, a decision tree analysis, is a machine learning method used for constructing predictive models from known data and is well established in the literature of ecological informatics (e.g., De'ath & Fabricius, 2000; Kulkarni & Shrestha, 2017; Moisen, 2008). Single input bands and SVIs were isolated from *Arundo* populations identified by TPWD (Figure 3) and served as the main predictors for the CART creation. The final model used Sentinel-2 bands 3 (Red), 4 (NIR), and NDVI as predictive variables. This model version has a generalized R2 of 0.76, meaning these variables account for 76% of *Arundo*'s predictability, and a cross validation R2 of 0.66, meaning there's a 66% agreement between predicted and observed classifications.

With the CART developed in JMP, a Python script was developed to run the model in ArcGIS Pro to apply the CART rules to Sentinel-2 imagery of training NFCAs. Accuracy assessment trips were organized based on equalized stratified random sampling of points classified as *Arundo* and non-*Arundo*. A total of 180 points (90 of each class) were initially created for model verification within training NFCAs. For the initial field-based accuracy assessment, 20 non-*Arundo* classified points and 47 *Arundo* classified points were evaluated via visual confirmation using binoculars or the sUAS for an alternative line-of-sight assessment. Visitation to the remaining randomly selected points were limited by landowner access denial and availability of safe sUAS launch locations. Once points were validated for true cover class (*Arundo* or non-*Arundo*), a confusion matrix of the model was organized to evaluate the model's classification accuracy.

OBJECTIVE 2: Expansion Rate Elucidation

The completed model in Objective 1 was applied to historic Sentinel-2 imagery of Stage 2 NFCAs (Figure 1) from 2015, 2018, and 2021 for elucidation of *Arundo*'s presence and regional expansion rate. Years were chosen to encompass the collection history of the satellite as it was deployed in 2015 and 2021 will have the most recent imagery. Sentinel-2A imagery acquisition and preparation followed the same workflow as described in Objective 1. Anticipated error of seasonal and atmospheric differences was mitigated by selecting imagery collection dates comparable to the dates of imagery used in the model development.

After model application across all years, a change detection analysis was performed to identify pixels of *Arundo* establishment (presence) and expansion (increase in patch number or average patch size). ArcGIS Pro was used to calculate classified pixel counts across respective NFCAs. FRAGSTATS, an open source, pixel based spatial analysis program commonly used for investigation of patch dynamics (McGarigal et al., 2023), was used to calculate patch and class metrics with outputs like patch area, patch numbers, and common distances between detected patches. The program allows for computation specification, like the election to operate on a 4-neighbor or 8-neighbor pixel rule (Figure 4). For this investigation, we opted to use the 8-neighbor rule for

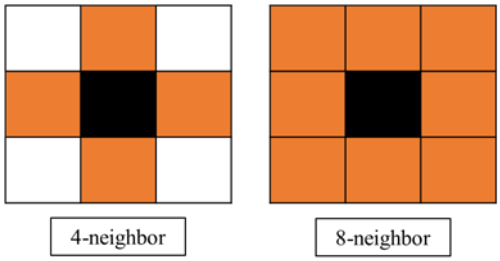

classification of a "patch" as *Arundo* morphometrics are highly variable and are likely to occur in diagonal pixels rather than strictly edge-sharing pixels. Using Stage 2 NFCA mapped models as inputs and selecting program parameters results in a summary of various patch and class metrics (see Table 6: Class Metrics; Table 7: Patch Metrics). Selected class metrics consisted of patch numbers and patch densities. Patch densities are reported as the number of patches per 100 hectares. A collection of pixels is referred to as a "patch" when they are adjacent or continuous based on the elected 8-neighor rule.

OBJECTIVE 3: Spatial Analyses to Identify Associated Landscape Features

The completed model in Objective 1 was planned to be used in spatial analysis to investigate relationships between landscape features and *Arundo* populations. Detected *Arundo* from 2022 imagery will be spatially related to key landscape features, such as wastewater treatment outfalls and proximity to roads or other built-up areas (Table 3). To accomplish this, attribute features were obtained from the respective data source, clipped to our 200m buffer extent of primary rivers, and projected to a unified coordinate system (WGS 1984/UTM Z 14N). With the approximate size of a given *Arundo* stand used as the predicted variable, distance to each of these features, measured through nearest neighbor statistics, were to be considered in a Gaussian Generalized Linear Regression to determine whether individual or combinations of landscape features coincide spatially with *Arundo* establishment. ArcGIS Pro was intended for use in this portion of analysis.

While investigating the landscape features associated with the presence of *Arundo* was a goal of this project, this objective was not completed. Complications arose during the model development and accuracy assessment stages of Objective 1. The resulting time limitation led us to prioritize addressing primary TPWD desires of Objective 1, creation of the 2022 *Arundo* inventory, and Objective 2, investigation of NFCA specific *Arundo* expansion. In addition, the poor accuracy of the majority of the eastern and western NFCAs made this analysis non-productive as any landscape feature associations found would likely not be reliable. Prepared data files will be provided to TPWD in the event an opportunity for agency completion arises.

Table 3: Examples of landscape features for investigation of correlation to *Arundo* presence. Landscape features, key attributes, and source of data are included for clarity.

	Landscape Feature	Attributes	Data Source
1	**Soil Moisture**	Soil horizon surveys	National Cooperative Soil Survey, USDA
2	**Flood Risk**	Relative degree of flood frequency	USGS
3	**Soil Nutrients**	Reported C:N ratios	National Cooperative Soil Survey, USDA
4	**Nutrient Input**	% Agricultural landcover in NFCA	TPWD Ecological Mapping System
		Distance to wastewater treatment facilities	TCEQ
5	**Anthropogenic Effects**	% Urban cover in NFCA	National Land Cover Database, USGS
		Distance to urban areas	National Land Cover Database, USGS
		Distance to roads	TxDOT
6	**Established *Arundo***	% *Arundo* landcover in NFCA	Created in Stage 1
		# Established *Arundo* stands in NFCA	Created in Stage 1

Results:

OBJECTIVE 1

Initial field-based accuracy assessments yielded an overall accuracy of 71% and a kappa value of 0.46 within training NFCAs of SEP and GUAD (Table 4). The overall accuracy indicates that 71% of pixels within this training area were correctly classified as *Arundo* or non-*Arundo*. The Kappa coefficient of agreement value of 0.46 indicates that the model has moderate agreement compared to chance alone. Satisfied with the detection accuracy, the Python script of the CART model rules was applied to Stage 1 NFCAs with ArcGIS Pro (Figure 5a). *Arundo* is reported most frequently along urban or suburban areas with intersecting river systems, while less developed areas have fewer classified pixels of *Arundo*.

Table 4: Field based accuracy assessment of SEP and GUAD training NFCAs.

	Actual		
Classified	*Non-Arundo*	*Arundo*	*Total*
Non-Arundo	16	4	20
Arundo	37	10	47
Total	53	14	67

Producer Accuracy	0.714
User Accuracy	0.213
Overall Accuracy	0.388
Kappa	0.460

Field-based accuracy assessments were initially performed in western and eastern NFCAs with equalized, randomly stratified samples of 60 points per class, however, the accessibility of survey points limited the success of these multi-week regional assessment trips. To account for this, independent computer-based accuracy assessments were instead performed for individual NFCAs to validate detection accuracy across a broad, geographically variable area. Computer-based accuracy assessments were conducted by comparing classified outputs to publicly assessable satellite imagery (e.g., Google Earth Pro). For simplicity, West Texas NFCAs of Pecos and Devils Rivers were grouped, as were East Texas NFCAs of the Northeast Texas Rivers and Southeast Texas River NFCAs.

Metrics of accuracy validation for individual or paired NFCAs were suboptimal despite several iterations of CART rule adjustments (Table 5; Figure 5b; Figure S2). Kappa values for the remote accuracy assessment across individual and paired NFCAs failed to reach even 0.10, which is interpreted as poor agreement. This led to the omission of most NFCAs from Objective 2. Future iterations of the predictive mapping methodology may be improved and would facilitate a broader area available for expansion rate analysis as detection accuracy improves. Our discussion supporting the incorporation of more fine spatial resolution imagery and the consideration of regionally based training imagery collection is included later in the discussion section for consideration.

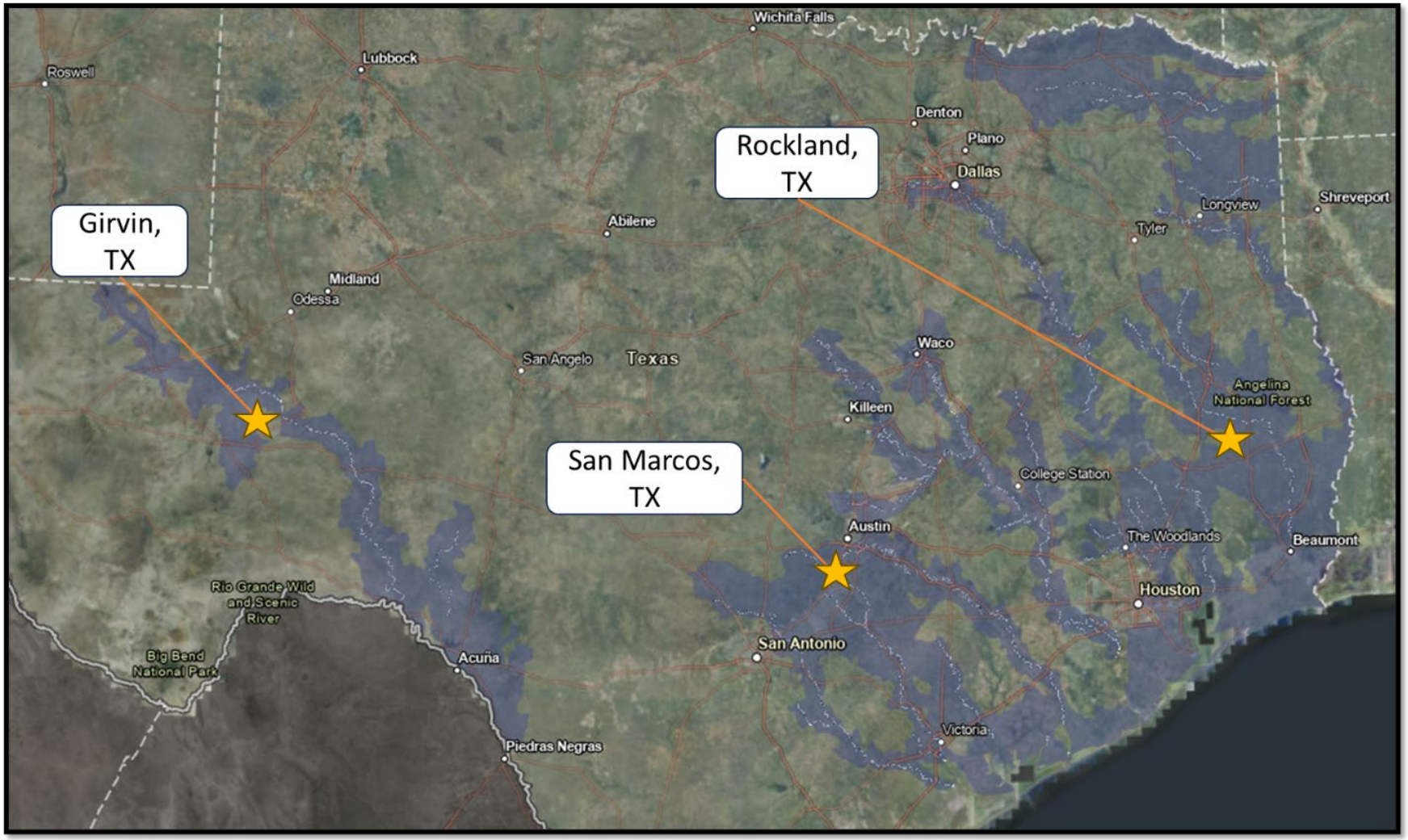

Figure 5(a): 2022 *Arundo* inventory across Stage 1 NFCAs identified by TPWD as areas of interest. Starred locations are displayed in more detail in Figure 5(b).

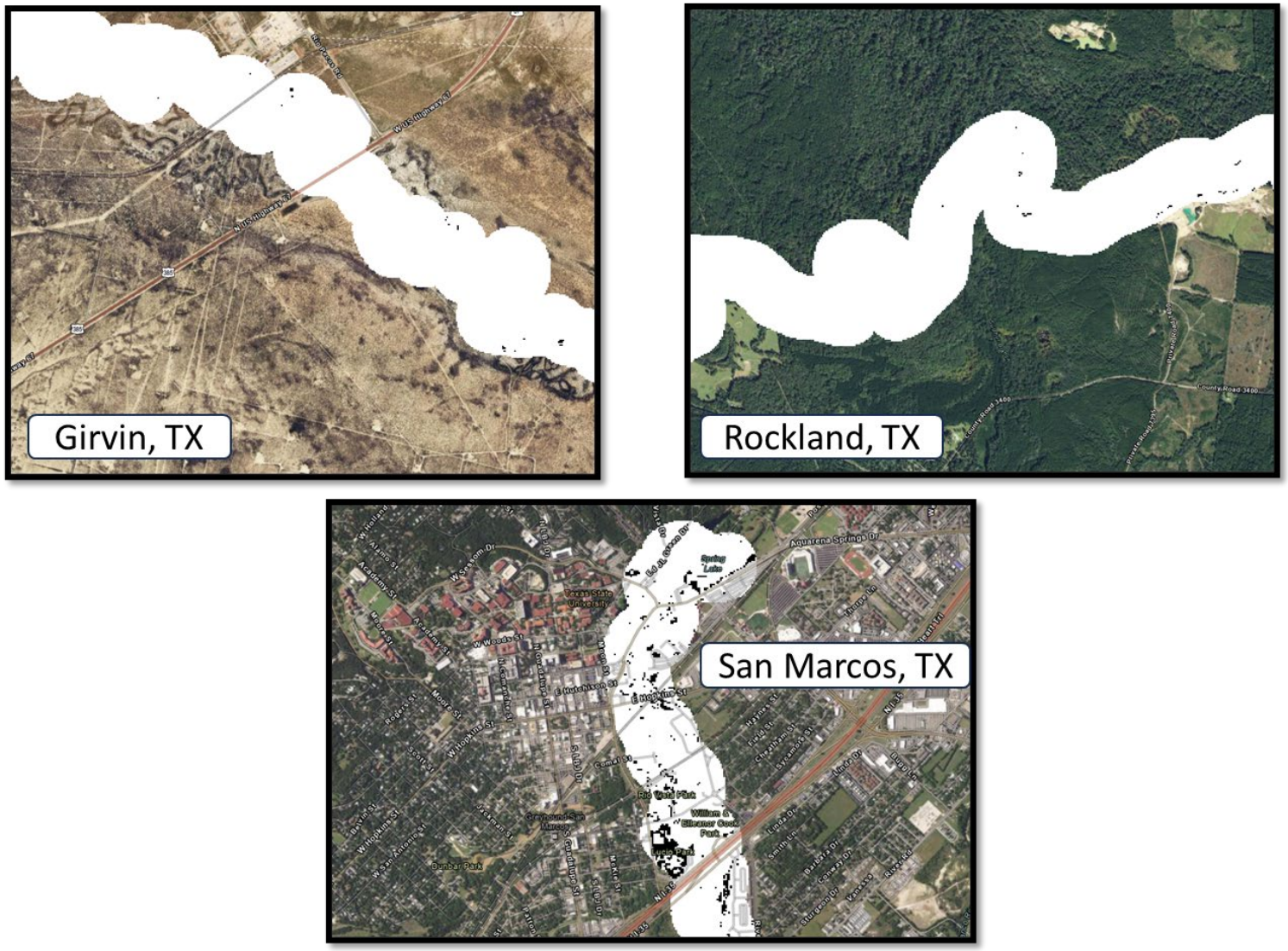

Figure 5(b): Output examples from West Texas (Girvin, Pecos River NFCA), Central Texas (San Marcos, Guadalupe and San Antonio Rivers NFCA), and East Texas (Rockland, Southeast Texas Rivers NFCA). White = non-*Arundo* Classification. Black = *Arundo* Classification.

Table 5: Confusion matrices of other (not GUAD or SEP) NFCAs. 5(a) belongs to the Lower Brazos, 5(b) to Mid-Brazos, 5(c) to Lower Colorado, 5(d) to San Gabriel, 5(e) to the Central Gulf Tributaries. 5(f) and 5(g) grouped Western and Eastern Texas NFCAs, respectively.

Lower Brazos	**Actual**		
Classified	*Non-Arundo*	*Arundo*	*Total*
Non-Arundo	40	0	40
Arundo	37	3	40
Total	77	3	80

Overall Accuracy	0.538
Producer Accuracy	0.519
User Accuracy	0.500
Kappa	0.036

5(a)

Lower Colorado	**Actual**		
Classified	*Non-Arundo*	*Arundo*	*Total*
Non-Arundo	40	0	40
Arundo	40	0	40
Total	80	0	80

Overall Accuracy	0.500
Producer Accuracy	0.500
User Accuracy	0.500
Kappa	0.000

5(c)

Central Gulf Tributaries	**Actual**		
Classified	*Non-Arundo*	*Arundo*	*Total*
Non-Arundo	40	0	40
Arundo	39	1	40
Total	79	1	80

Overall Accuracy	0.513
Producer Accuracy	0.506
User Accuracy	0.500
Kappa	0.012

5(e)

Mid-Brazos	**Actual**		
Classified	*Non-Arundo*	*Arundo*	*Total*
Non-Arundo	40	0	40
Arundo	39	1	40
Total	79	1	80

Overall Accuracy	0.513
Producer Accuracy	0.506
User Accuracy	0.500
Kappa	0.012

5(b)

San Gabriel	**Actual**		
Classified	*Non-Arundo*	*Arundo*	*Total*
Non-Arundo	40	0	40
Arundo	40	0	40
Total	80	0	80

Overall Accuracy	0.500
Producer Accuracy	0.500
User Accuracy	0.500
Kappa	0.000

5(d)

East Texas NFCAs	**Actual**		
Classified	*Non-Arundo*	*Arundo*	*Total*
Non-Arundo	72	0	72
Arundo	69	0	69
Total	141	0	141

Overall Accuracy	0.511
Producer Accuracy	0.511
User Accuracy	0.511
Kappa	0.000

5(f)

West Texas NFCAs	**Actual**		
Classified	*Non-Arundo*	*Arundo*	*Total*
Non-Arundo	60	0	60
Arundo	56	4	60
Total	116	4	120

Overall Accuracy	0.533
Producer Accuracy	0.517
User Accuracy	0.533
Kappa	0.067

5(g)

OBJECTIVE 2

ArcGIS Pro's Change Detection Wizard outputs are summarized in Table 6. Coverage of non-*Arundo* and *Arundo* classes are reported along with total area of the respective NFCA. For visual representation (Figure 6), changes from non-*Arundo* classification to *Arundo* classification are shown as red, while changes from *Arundo* to non-*Arundo* are shown as black against a yellow area of interest (AOI) backdrop. The yellow background depicts the buffered river AOI. This is an overview from 2015 to 2021 within SEP to capture the range of years.

Table 6: SEP (left) and GUAD (right) expansion calculation (km2).

	2015	2018	2021
Non-Arundo	13.402	13.473	13.123
Arundo	0.001	0.013	0.229
Total Area	13.403	13.486	13.352
%Arundo	0.011	0.095	1.715

2015 - 2018 Expansion Rate
0.028% gain per year
2018 - 2021 Expansion Rate
0.54% gain per year
Overall Expansion Rate
0.284% gain per year

	2015	2018	2021
Non-Arundo	39.411	39.495	39.503
Arundo	0.122	0.037	0.087
Total Area	39.533	39.532	39.59
%Arundo	0.003	0.001	0.002

2015 - 2018 Expansion Rate
0.0000067% loss per year
2018 - 2021 Expansion Rate
0.00033% gain per year
Overall Expansion Rate
0.00015% loss per year

SEP expansion from 2015 – 2018 had a 0.028% gain per year for *Arundo* cover, though this increased between 2018 – 2021 to a 0.54% yearly gain (Table 6). As this area was exiting the drought of 2015, this gain was anticipated as *Arundo* is highly reliant on freshwater availability. The overall expansion rate of 0.284% per year within SEP indicates class coverage of *Arundo* increasing. GUAD expansion from 2015 – 2018, on the other hand, experienced a 0.0000067% loss per year of *Arundo* cover, shifting to a gain of 0.00033% per year between 2018 -2021 (Table 6). The initial loss in GUAD may be attributed to a lag effect of drought impacts remaining from 2015, though communication with professional contacts at TPWD led us to attribute the loss of *Arundo* in this NFCA at an overall rate of 0.015% per year with TPWD management efforts rather than any environmental factors or decreasing *Arundo* fitness.

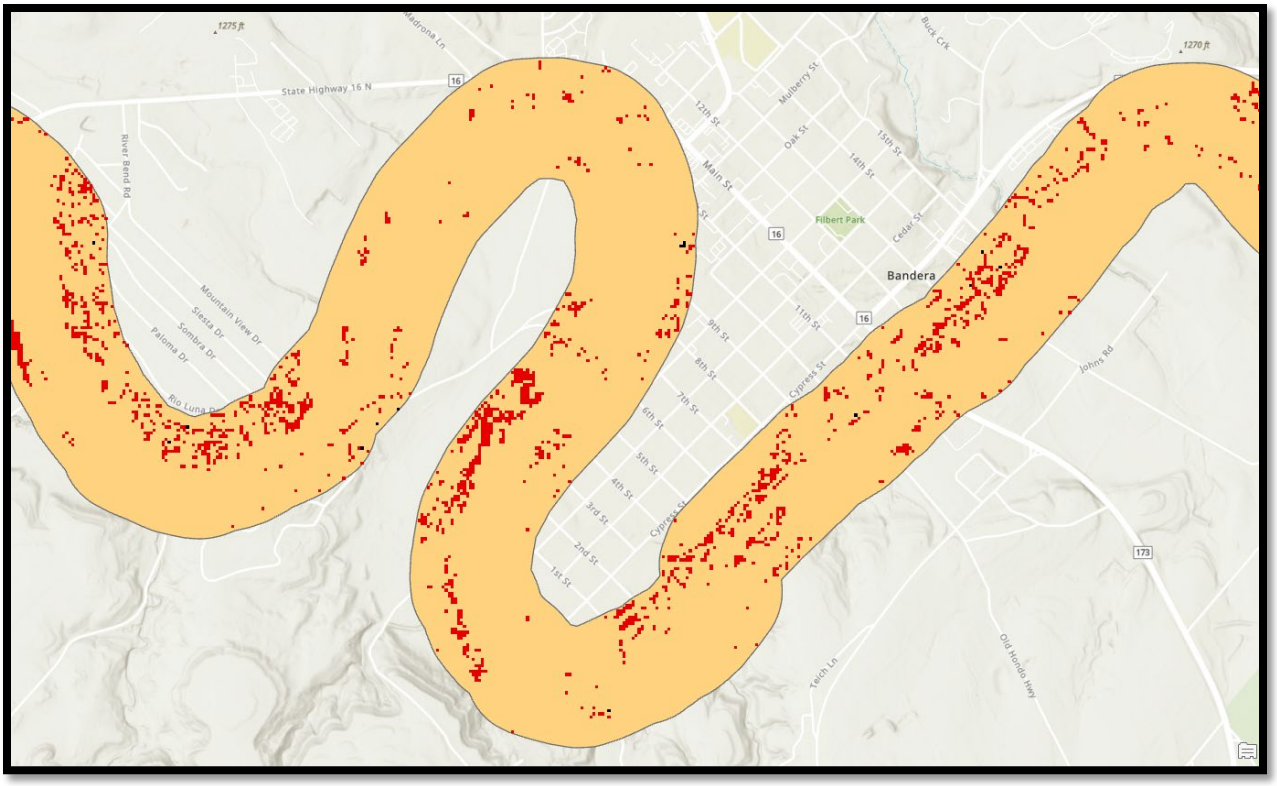

Figure 6: Excerpt from Bandera, Texas. Output from SEP 2015-2021 Change Detection Wizard in ArcGIS Pro.
Red = Non-*Arundo* -> *Arundo*
Black = *Arundo* -> Non-*Arundo*

Table 7: FRAGSTATS class metric outputs based on 8-neighbor pixel rule. Patch density output to be read as the number of patches per 100 hectares.

		SEP		GUAD	
		#patches	*patch density*	*#patches*	*patch density*
2015	*Arundo*	122	0.914	3351	8.477
2018	*Arundo*	891	6.611	1505	3.807
2021	*Arundo*	5888	44.125	1885	4.761
		SEP		**GUAD**	
		#patches	*patch density*	*#patches*	*patch density*
2015	*Non-Arundo*	10	0.075	35	0.089
2018	*Non-Arundo*	4	0.030	16	0.041
2021	*Non-Arundo*	75	0.562	24	0.061

Table 8: Summary of FRAGSTATS patch metrics output of annual patch area. Default reporting units are hectares.

	SEP		GUAD	
	avg. patch area	*std.dev*	*avg. patch area*	*std.dev*
2015	0.012	0.005	1.155	0.364
2018	0.014	0.031	0.024	0.078
2021	0.039	0.089	0.046	0.139

FRAGSTAT summarization of class metrics (Table 7) reports number of patches and average density of patches across the three years of our expansion rate investigation within Stage 2 NFCAs AOI. SEP patch numbers increase quickly and consistently, while GUAD patch numbers decreased sharply between 2015 and 2018. This seems to have been followed by a regain of patch numbers between 2018 and 2021.

FRAGSTAT summarization of patch metrics (Table 8) reports the average patch areas for each year with standard deviations as measures of variability. A patch area of 0.01 hectare = 100 m^2 agrees with our 10 x10 m pixel area of a single, isolated pixel of classified *Arundo*. With this interpretation, most patch area averages across these years of investigation only consist of a handful of adjacent, isolated *Arundo* classified pixels. Large ranges of standard deviations indicate a high level of patch size variability, though, attributed with *Arundo*'s opportunistic growth pattern that takes advantage of canopy gaps and bare soils for root establishment. The gradual increase in average patch areas for SEP and increasing standard deviation show that patches are growing across the landscape with relatively inconsistent area. GUAD average patch areas, though, shows an initial decrease followed by a partial regrowth. This pattern suggests a die back of *Arundo* across GUAD that was followed by additional growth in the following years.

Discussion:

SEP and GUAD NFCAs, where the model performed acceptably, were visually assessed. While there are frequent isolated pixels of *Arundo* classifications across the landscape, it appears as though most *Arundo* occurrences are present in sub-urban, and likely built-up locations. The buildup of sub-urban housing areas is often performed by importing soil from other regions with the intent of mitigating the potential for property loss during flood events. Where the AOI of our buffered rivers approached city centers (e.g., San Antonio, Bandera, and San Marcos), occurrence of *Arundo* seem to increase in density. This aligns with in-field observations where larger *Arundo* stands were mostly observed along roadsides of well-traveled highways or river sections where banks indicated frequent flooding suggested by the absence of established woody species and abundance of bare soil patches. This also suggests that in less developed areas *Arundo* is less of a problem and may not warrant as much management action.

Though our detection accuracy for the SEP and GUAD area is approximately 71%, there are portions of this region that are suspected of inadequate model performance. Most training samples were gathered from the eastern extent of SEP and the western extent of GUAD, influenced by known *Arundo* locations from TPWD. During the early stages of the initial model development, classifications to the east of Interstate 35 greatly overclassified *Arundo*. While

following iterations improved this overclassification, similar overclassification may be increasing proportionately with distance from our training locations.

Completion of the remote sensing based *Arundo* inventory of 2022 was not without challenges, though, as only SEP and GUAD reached acceptable confidence levels. Initial collection of sUAS imagery was complicated by private land restrictions and limited knowledge of locations of established *Arundo* by TPWD. With an estimated 93% of Texas land being privately owned and landowners often reluctant to engage in management practices without compensation (Kreuter et al., 2006; Texas Parks and Wildlife Department, n.d.), imagery collection was restricted to public access roads within a safe flight range of the sUAS. While this is permissible by law as air space is not privately owned, members of the field team were strongly encouraged to use strategies to prevent negative community interaction that could negatively impact TPWD's Healthy Creeks Initiative efforts for community engagement. The goal of this landowner outreach was to encourage landowner involvement, respect landowner privacy concerns, and conduct research with transparency. Initial outreach was attempted using county appraisal district address records to call or email landowners prior to flights and, if contact attempts failed as they often did, the field crew carried and distributed notification fliers to landowners.

Furthermore, the variation of phenotypic seasonality for *Arundo* was of noted concern during the planning stage. From personal observations, *Arundo* appears conspicuous from mid-summer after spring rains, to late fall before multi-day freezes. *Arundo'*s characteristically large inflorescences, visible in sUAS imagery, have been observed from mid-summer to late fall before stands senesce. Noting the seasonality of *Arundo* is valuable in that quality, high-resolution imagery collection of conspicuous *Arundo* stands is needed for calculation of *Arundo* specific spectral responses to reduce risk of mixed, or "impure", pixel values. Other projects using remote sensing for species specific detections found significant spatial variability of their study species within coarse satellite imagery (Sha et al., 2008; Sharp et al., 2021). For example, Sharp et al. (2021) found that the Critical Scale of Variability (CSV) for their focal cyanobacteria ranged from 70 to 175 m. CSVs summarize the recommended distance across a landscape required between samples to capture independent, representative values of spatial patchiness or densities of patches. As the project was working with 300 m coarse resolution satellite imagery, high spatial variability of detected cyanobacteria blooms was reported within each pixel. The high variability within coarse pixel imagery was suggested to have been the primary limitation in creating a modeled algorithm capable of accurate remote detection of cyanobacteria within Sharp's study area. Similar remote sensing-based approaches attributes the complication of identifying pure, species-specific SVIs to impure spectral responses, suggesting that high resolution imagery is best suited for species-specific remote detection (Cingolani et al., 2004). Success of other study's detection efforts commonly use high spatial resolution imagery for the identification of singular or multiple study species, which is commonly referenced for the advocation of selecting high-resolution imagery for species-specific detection studies (Hill et al., 2017; Lass et al., n.d.; Mu et al., 2023). For improved products meant to assist managers, TPWD members should advocate for a subscription to a high-resolution imagery acquisition organization. Our study was limited by the moderately coarse spatial resolution of 10 m and 20 m Sentinel-2 pixels that was publicly available, leading us to primarily emphasize 10 m pixels and 10 m resampled pixels with >50% *Arundo* canopy cover. Use of a higher spatial resolution, at least sub-10 m, should yield more accurate classification results and will benefit the identification of species of interest for TPWD management efforts.

In addition to these struggles, Sentinel-2's spatial resolution of 10 m – 20 m pixels resulted in expected mixed pixel values. Mixed pixels consist of "impure" spectral responses (example: *Arundo* and non-*Arundo* vegetation) and can be difficult to accurately classify (Figure 7). While adjustments of statistical parameters in the CART analysis were performed across several iterations to improve detection accuracy and reduce error, there is no attainable method of entirely removing errors attributed to mixed pixels (Boonprong et al., 2017). Use of higher spatial resolution imagery is most recommended to avoid this error source (Cingolani et al., 2004). The errors attributed to mixed pixel values in this study have been captured in the final model's regional accuracy assessment where a detection rate of 71% was accepted.

Compared to a preceding remote sensing study performed in 2003 by Everitt et al. (2004), our detection rate was suboptimal. Everitt et al. utilized Quickbird satellite imagery at 2.8 m spatial resolution for the detection of *Arundo donax* within a portion of the Rio Grande Valley near Del Rio, Texas. Though imagery acquisition costs approximately $1900 for 64 km^2 area, this high-resolution imagery was successfully manipulated to detect *Arundo* with 83% accuracy and a strong kappa of 0.77 using false color satellite imagery band combinations and a 79% accuracy and kappa of 0.724 using true color band combinations (Everitt et al., 2004). False color refers to using green, red, and near-infrared bands while true color combinations consist of a red, green, and blue band combination. Despite having the same focal species and performing our studies in the same state, there are several key differences between our project methodologies. First, Everitt et al.'s funding allowed for the purchase of 2.8 m high spatial resolution imagery, whereas our study emphasized open-access imagery sources. Second, different satellite sensors were used. The Quickbird satellite was decommissioned in 2015 after experiencing orbital decay – this coincidentally aligns with the launch of Sentinel-2 in 2015, which was ultimately selected due to recent and ongoing operation. Third, Everitt et al.'s study scope did not evaluate the utility of applying detection rules in a relatively small area to a broader, more expansive geographic scale across various ecoregions of the state.

Figure 7: South of Medina, Texas. 2015-2018 Change Detection Wizard overlayed, where red pixels denote classified *Arundo*. Note that some pixels contain non-Arundo like herbaceous and woody species, as well as developed lands.

Finally, we opted to use SVI calculations as a primary detection metric rather than spectral combinations of true or false color imagery. Though it is encouraging that more accurate detection methods have been documented in this way, more work must be done to improve the statewide detection of *Arundo* across various vegetative communities and soil types using SVIs that are more reliable for species-specific remote detection (Xie et al., 2008).

Application of the trained model to such a large land area was expected to increase overall map uncertainty. To reduce this, additional clipping of the study areas focused

specifically on banks of non-ephemeral, classified streams and rivers. Similar studies investigating the use of remote sensing along river corridors for species specific spectral identification, though, have documented increased fragmentation and diminished accuracy with use of medium to coarse imagery resolution (Congalton et al., 2002; Gergel et al., 2007; Henshaw et al., 2013). Again, this error may be mitigated by using higher spatial resolution imagery for investigation, though large maps are often critiqued to overestimate model predictive power (Ploton et al., 2020; Tan et al., 2006). For these reasons, the production of regional maps for species detection may be in the best interest of any statewide management group for Texas.

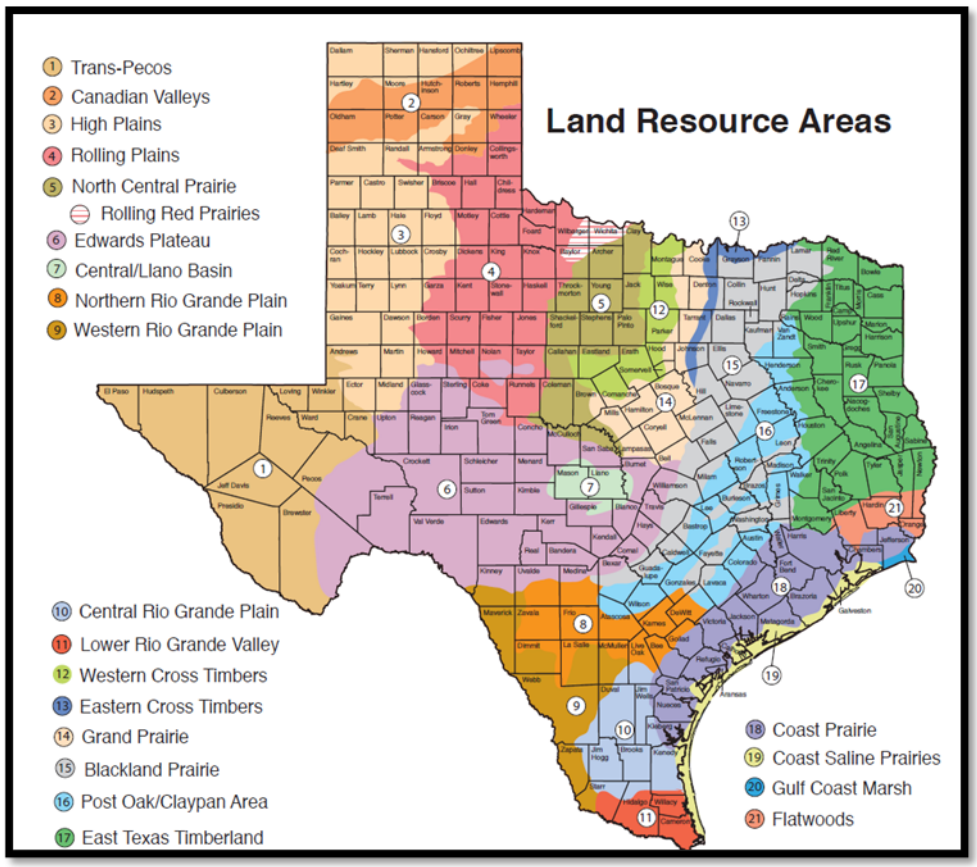

Figure 8: Land Resource Areas created by Texas Almanac (Texas Almanac Graphic, n.d.). Classifications largely based on soil types as sourced from the Natural Resources Conservation Service of the U.S. Department of Agriculture. Compare to Figure 4 for understanding of focal NFCA coverage.

Additionally, Texas' variable landscape likely complicated accurate remote detection. Soil reflectance, largely attributed to soil moisture, is expected to greatly vary between western and eastern NFCAs where landscapes shift from arid desert environments to swampy wetlands (Texas Almanac, 2021) (Figure 8). While these concerns can be managed to respectively correct spatial-temporal discrepancies and spectral overlaps, we acknowledge these as anticipated sources of error. After the encountered complications with improving detection accuracy of the

model, we would further recommend collecting training sUAS imagery across multiple regions of your study's scope. Individual models organized by region should yield more accurate results.

Conclusion:

This project provides a framework for continued remote sensing-based detection methods of a conspicuous invasive species of significant habitat management concern within Texas NFCAs. Though there were issues with model accuracy, this is the first attempt at creating fully remote sensing-based inventory of *Arundo* along with evaluation of expansion rates within Central Texas NFCAs. While we addressed complications encountered and sources of expected error, this project does supplement knowledge gaps regarding expansion characteristics of *Arundo* within Central Texas. It is our hope that the methods and recommendations included in this report will be incorporated into TPWD's ongoing *Arundo* management efforts. Continued mapping of the species will provide agencies with a more complete picture of how widespread invasions have become within NFCAs, along with how the invasion has spread in this 7-year time span. A more robust analysis may stem from this methodology for a more complete consideration of influential landscape features contributing to infestations. This will help in identifying what biotic and abiotic factors are commonly associated with invasion success in this region. Additional landscape features such as adjacency to established *Arundo* stands, soil moisture, and nutrient inputs are acknowledged as influential, and should be incorporated in future investigations to elucidate local contributors to *Arundo* invasions in Central Texas. Upon visual inspection, it appears as though *Arundo* is most concentrated around built-up suburban centers and low river crossings prone to flood events. Incorporation of these data into future landscape analysis should allow for more accurate prediction of habitats at high invasion risk. This should facilitate greater efficiency in priority assignment and implementation of proactive management.

Management Implications:

Our project lays the groundwork for future mapping projects that could lead to significant management outcomes for *Arundo* (e.g., current *Arundo* project support, future project targeting) as well as the conservation implications (e.g., guiding management to restore critical habitat, focusing on NFCAs). Our research project focused both on established, problematic infestations where restoration is currently ongoing and recent stand expansions or reductions in those areas. Though identification of priority NFCAs for management action was not able to be completed in this project due to low accuracy of the remote sensing products outside of central Texas, it is clear that with the purchase and incorporation of higher resolution imagery and regional specific training model development products could be created that would be essential to identify NFCAs across Texas where management efforts should be focused.

Based on TPWD's goals of controlling *Arundo* invasion and spread, there remains a need to know where successful populations of *Arundo* are located throughout NFCAs. The land area occupied by NCFAs is too large to monitor with boots on the ground and requires a remote sensing approach to be able to identify and respond to *Arundo* invasions. The methods that we developed as part of this project lay out a data processing path that could be useful to TPWD in the future if higher resolution imagery is available to locate infestations in NFCAs throughout Texas. While the landscape factors spatial analysis of this project was unable to be completed, it is very likely, based on past studies, that *Arundo*'s successful invasion across the landscape, both in terms of total size of the infestation and rate of patch spread, is due to both biotic (e.g.,

proximity to other *Arundo* stands) and abiotic factors (e.g., soil moisture, nutrient inputs, etc.). Gaining a better understanding of these factors would allow TPWD to better predict the sites where *Arundo* will establish and more efficiently implement management strategies in priority areas. We strongly suggest TPWD invest in both higher resolution imagery and future analyses into the landscape features most associated with *Arundo* dominance. In addition, the inclusion of regionally specific training flights with additional personnel and funding availability would further enhance the likelihood of being able to accurately identify *Arundo* at large regional scales.

Though imperfect, our project resulted in the first remote sensing-based inventory of *Arundo* presence within two NFCAs in Texas and clear methodology and operational model for TPWD to continue detection efforts in the future with high resolution, commercially available satellite imagery.

Literature Cited:

Able, K. W., & Hagan, S. M. (2003). Impact of common reed, *Phragmites australis*, on essential fish habitat: influence on reproduction, embryological development, and larval abundance of mummichog (*Fundulus heteroclitus*). *Estuaries*, *26*(1), 40-50.

Ahmad, R., Liow, P. S., Spencer, D. F., & Jasieniuk, M. (2008). Molecular evidence for a single genetic clone of invasive *Arundo donax* in the United States. *Aquatic Botany*, *88*(2), 113-120.

Bell, G.P. (1997). Ecology and management of *Arundo donax*, and approaches to riparian habitat restoration in southern California. In: Brock, J. H.; Wade, M.; Pysek, P.; Green, D., eds. Plant invasions: studies from North America and Europe. Leiden, The Netherlands: Backhuys Publishers: 103-113. [43820]

Boland, J. M. (2006). The Importance of Layering in the Rapid Spread of *Arundo* donax (Giant Reed). *Madroño*, *53*(4), 303–312. https://doi.org/10.3120/0024-9637(2006)53[303:tiolit]2.0.co;2

Boland, J.M. (2008). The Roles Of Floods And Bulldozers In the Break-Up and Dispersal Of *Arundo donax* (Giant Reed). Madroño, 55(3), 216-222.

Boonprong, S., Cao, C., Torteeka, P., & Chen, W. (2017). A novel classification technique of Landsat-8 OLI image-based data visualization: The application of Andrews' plots and fuzzy evidential reasoning. *Remote Sensing*, *9*(5). https://doi.org/10.3390/rs9050427

Cingolani, A. M., Renison, D., Zak, M. R., & Cabido, M. R. (2004). Mapping vegetation in a heterogeneous mountain rangeland using landsat data: An alternative method to define and classify land-cover units. *Remote Sensing of Environment*, *92*(1), 84–97. https://doi.org/10.1016/j.rse.2004.05.008

Congalton, R., Birch, K., Jones, R., & Schriever, J. (2002). Evaluating Remotely Sensed Techniques for Mapping Riparian Vegetation. *Computers and Electronics in Agriculture*, *37*, 113–126. https://doi.org/10.1016/S0168-1699(02)00108-4

Curt, M., Mauri, P., Sanz, M., Cano-Ruiz, J., del Monte, J., Aguado, P. and Sánchez, J., (2017). The ability of the *Arundo donax* crop to compete with weeds in central Spain over two growing cycles. Industrial Crops and Products, 108, 86-94.

Cushman, J. H., & Gaffney, K. A. (2010). Community-level consequences of invasion: impacts of exotic clonal plants on riparian vegetation. Biological Invasions, 12(8), 2765–2776.

De'ath, G., & Fabricius, K. E. (2000). Classification and Regression Trees: A Powerful Yet Simple Technique for Ecological Data Analysis. In *Ecology* (Vol. 81, Issue 11).

Decruyenaere, J. G., & Holt, J. S. (2001). Seasonality of clonal propagation in giant reed. Weed Science, 49(6), 760–767.

Di Mola, I., Guida, G., Mistretta, C., Giorio, P., Albrizio, R., Visconti, D., Fagnano, M., & Mori, M. (2018). Agronomic and physiological response of giant reed (*Arundo donax* L.) to soil salinity. Italian Journal of Agronomy, 13(1), 31.

Escutia-Lara, Y., Gomez-Romero, M., & Lindig-Cisneros, R. (2009). Nitrogen and phosphorus effect on *Typha domingensis* Presl. Rhizome growth in a matrix of *Schoenoplectus americanus* (Pers.) Volkart ex Schinz and Keller. Aquatic Botany, 90(1), 74-77.

Everitt, J. H., Yang, C., & Deloach, C. J. (2004). Remote sensing of giant reed with QuickBird satellite imagery Image debating based on improved dark channel prior method for agriculture View project Remote Sensing of Giant Reed with QuickBird Satellite Imagery. In *Article in Journal of Aquatic Plant Management* (Vol. 43). https://www.researchgate.net/publication/43287873

Gergel, S. E., Stange, Y., Coops, N. C., Johansen, K., & Kirby, K. R. (2007). What is the value of a good map? An example using high spatial resolution imagery to aid riparian restoration. *Ecosystems*, *10*(5), 688–702. https://doi.org/10.1007/s10021-007-9040-0

Gitelson, A., & Merzlyak, M. N. (1994). Quantitative estimation of chlorophyll-u using reflectance spectra: experiments with autumn chestnut and maple leaves. In *J. Photochem. Photobiol. B: Bioi* (Vol. 22).

Gitelson, A., Merzlyak, M.N., 1994. Quantitative estimation of chlorophyll-a using reflectance spectra - experiments with autumn chestnut and maple leaves. J.Photochem. Photobiol. B Biol. 22, 247–252.

Green, E. K., & Galatowitsch, S. M. (2001). Differences in wetland plant community establishment with additions of nitrate-N and invasive species (*Phalaris arundinacea* and *Typha× glauca*). Canadian Journal of Botany, 79(2), 170-178.

Goolsby, J. A., Moran, P. J., Racelis, A. E., Summy, K. R., Jimenez, M. M., Lacewell, R. D., ... & Kirk, A. A. (2016). Impact of the biological control agent *Tetramesa romana* (Hymenoptera: Eurytomidae) on *Arundo* donax (Poaceae: Arundinoideae) along the Rio Grande River in Texas. Biocontrol Science and Technology, *26*(1), 47-60.

Hardion, L., Verlaque, R., Saltonstall, K., Leriche, A. and Vila, B., (2014). Origin of the invasive *Arundo donax* (Poaceae): a trans-Asian expedition in herbaria. Annals of Botany, 114(3), 455-462.

Henshaw, A., Gurnell, A., Bertoldi, W., & Drake, N. (2013). An assessment of the degree to which Landsat TM data can support the assessment of fluvial dynamics, as revealed by changes in vegetation extent and channel position, along a large river. *Geomorphology*, *202*, 74–85. https://doi.org/10.1016/j.geomorph.2013.01.011

Herod, M. and J.P. Martina. 2023. Environmental factors influencing the growth and resource allocation of *Arundo donax*, a riparian invader. *Weed Research* 1-11

Herrera, A. M., & Dudley, T. L. (2003). Reduction of riparian arthropod abundance and diversity as a consequence of giant reed (*Arundo donax*) invasion. Biological Invasions, 5(3), 167-177.

Hill, D. J., Tarasoff, C., Whitworth, G. E., Baron, J., Bradshaw, J. L., & Church, J. S. (2017). Utility of unmanned aerial vehicles for mapping invasive plant species: a case study on yellow flag iris (Iris pseudacorus L.). *International Journal of Remote Sensing*, *38*(8–10), 2083–2105. https://doi.org/10.1080/01431161.2016.1264030

Jain, S., Ale, S., Munster, C., Ansley, R., & Kiniry, J. (2015). Simulating the Hydrologic Impact of *Arundo donax* Invasion on the Headwaters of the Nueces River in Texas. Hydrology, 2(3), 134–147.

Kisner, D. A. (2004). The Effect of Giant Reed (*Arundo donax*) on the Southern California Riparian Bird Community. M.S. thesis. San Diego, CA: San Diego State University. 90 p.

Kreuter, U. P., Nair, M. V, Jackson-Smith, D., Conner, J. R., & Johnston, J. E. (2006). Property Rights Orientations and Rangeland Management Objectives: Texas, Utah, and Colorado. *Rangeland Ecol Manage*, *59*, 632–639.

Kulkarni, A., & Shrestha, A. (2017). Multispectral Image Analysis using Decision Trees. In *IJACSA) International Journal of Advanced Computer Science and Applications* (Vol. 8, Issue 6). www.ijacsa.thesai.org

Lambert, A. M., Dudley, T. L., & Saltonstall, K. (2010). Ecology and impacts of the large-statured invasive grasses *Arundo donax* and *Phragmites australis* in North America. Invasive Plant Science and Management, 3(4), 489-494.

Lass, L. W., Carson, H. W., & Callihan, R. H. (n.d.). Detection of Yellow Starthistle (Centaurea solstitialis) and Common St. Johnswort (Hypericum perforatum) with Multispectral Digital Imagery. In *Technology* (Vol. 10, Issue 3). https://www.jstor.org/stable/3988139

Mangla, S., Sheley, R. L., James, J. J., & Radosevich, S. R. (2011). Intra and interspecific competition among invasive and native species during early stages of plant growth. Plant Ecology, 212(4), 531–542

Mariani, C., Cabrini, R., Danin, A., Piffanelli, P., Fricano, A., Gomarasca, S., Dicandilo, M., Grassi, F., & Soave, C. (2010). Origin, diffusion and reproduction of the giant reed (*Arundo* donax L.): A promising weedy energy crop. *Annals of Applied Biology*, *157*(2), 191–202. https://doi.org/10.1111/j.1744-7348.2010.00419.x

Martina, J. P., & von Ende, C. N. 2012. Highly plastic response in morphological and physiological traits to light, soil-N and moisture in the model invasive plant, *Phalaris arundinacea*. Environmental and Experimental Botany, 82, 43–53.

Martina, J.P., Currie, W.S., Goldberg, D.E., and K.L. Elgersma. 2016. Nitrogen loading leads to increased carbon accretion in both invaded and uninvaded coastal wetlands. Ecosphere 7(9): e01459. 10.1002/ec2.1459.

McGarigal, Kevin; Marks, Barbara J. 1995. Fragstats: spatial pattern analysis program for quantifying landscape structure. Gen. Tech. Rep. PNW-GTR-351. Portland, OR: U.S. Department of Agriculture, Forest Service, Pacific Northwest Research Station. 122 p.

Minchinton, T. E., & Bertness, M. D. (2003). Disturbance-mediated competition and the spread of *Phragmites australis* in a coastal marsh. Ecological Applications, 13(5), 1400-1416.

Moisen, G. G. (2008). Classification and regression trees. *In: Jørgensen, Sven Erik; Fath, Brian D. (Editor-in-Chief). Encyclopedia of Ecology, volume 1. Oxford, UK: Elsevier. p. 582-588.*, 582-588.

Moore, G. W., Watts, D. A., & Goolsby, J. A. (2010). Ecophysiological responses of giant reed (*Arundo donax*) to herbivory. Invasive Plant Science and Management, 3(4), 521-529.

Mu, S., You, K., Song, T., Li, Y., Wang, L., & Shi, J. (2023). Identification for the species of aquatic higher plants in the Taihu Lake basin based on hyperspectral remote sensing. *Environmental Monitoring and Assessment*, *195*(8). https://doi.org/10.1007/s10661-023-11523-z

Nackley, L., Hough-Snee, N., & Kim, S.-H. (2017). Competitive traits of the invasive grass *Arundo donax* are enhanced by carbon dioxide and nitrogen enrichment. Weed Research, 57(2), 67–71.

Perdue, R. E. (1958). *Arundo donax*—Source of musical reeds and industrial cellulose. Economic Botany, 12(4), 368–404

Ploton, P., Mortier, F., Réjou-Méchain, M., Barbier, N., Picard, N., Rossi, V., Dormann, C., Cornu, G., Viennois, G., Bayol, N., Lyapustin, A., Gourlet-Fleury, S., & Pélissier, R. (2020). Spatial validation reveals poor predictive performance of large-scale ecological mapping models. *Nature Communications*, *11*(1). https://doi.org/10.1038/s41467-020-18321-y

Quinn, L. D., & Holt, J. S. (2008). Ecological correlates of invasion by *Arundo donax* in three southern California riparian habitats. Biological Invasions, 10(5), 591–601.

Quinn, L. D., Rauterkus, M. A., & Holt, J. S. (2007). Effects of Nitrogen Enrichment and Competition on Growth and Spread of Giant Reed (*Arundo* donax). Weed Science, 55(4), 319–326.

Racelis, A. E., Davey, R. B., Goolsby, J. A., De León, A. P., Varner, K., & Duhaime, R. (2012). Facilitative ecological interactions between invasive species: *Arundo donax* stands as favorable habitat for cattle ticks (Acari: Ixodidae) along the US–Mexico border. Journal of medical entomology, 49(2), 410-417.

Rouse, J.W., Haas, R.H., Deering, D.W., Schell, J.A., & Harlan, J.C. (1974). "Monitoring Vegetation Systems in the Great Plains with ERTS,". In, *Proceedings, 3rd Earth Resource Technology Satellite (ERTS) Symposium*. pp. 48-62.

Sha, Z., Bai, Y., Xie, Y., Yu, M., & Zhang, L. (2008). Using a hybrid fuzzy classifier (HFC) to map typical grassland vegetation in Xilin River Basin, Inner Mongolia, China. *International Journal of Remote Sensing*, *29*(8), 2317–2337. https://doi.org/10.1080/01431160701408436

Sharp, S. L., Forrest, A. L., Bouma-Gregson, K., Jin, Y., Cortés, A., & Schladow, S. G. (2021). Quantifying Scales of Spatial Variability of Cyanobacteria in a Large, Eutrophic Lake Using Multiplatform Remote Sensing Tools. *Frontiers in Environmental Science*, *9*. https://doi.org/10.3389/fenvs.2021.612934

sugar maple leaves. *Int. J. Remote Sens*. 14, 1563–1575.

Tan, C. O., Özesmi, U., Beklioglu, M., Per, E., & Kurt, B. (2006). Predictive models in ecology: Comparison of performances and assessment of applicability. *Ecological Informatics*, *1*(2), 195–211. https://doi.org/10.1016/j.ecoinf.2006.03.002

Tarin, D., Pepper, A. E., Goolsby, J. A., Moran, P. J., Arquieta, A. C., Kirk, A. E., & Manhart, J. R. (2013). Microsatellites uncover multiple introductions of clonal giant reed (*Arundo donax*). Invasive Plant Science and Management, 6(3), 328-338.

Texas Almanac Graphic. (n.d.). *Land Resource Areas*.

Texas Almanac. (2021). *Soils of Texas*. Texas State Historical Association (TSHA). https://www.texasalmanac.com/articles/soils-of-texas#:~:text=The%20upland%20soils%20are%20mostly,is%20the%20major%20land%20use.

Texas Parks and Wildlife Department. (n.d.). *Private Land Owners and Listed Species*. Retrieved December 21, 2022, from https://tpwd.texas.gov/huntwild/wild/wildlife_diversity/nongame/listed-species/landowner-tools.phtml#:~:text=Texas%20is%20a%20private%20lands,we%20enjoy%20in%20our%20state

Tho, B. T., Lambertini, C., Eller, F., Brix, H., & Sorrell, B. K. (2017). Ammonium and nitrate are both suitable inorganic nitrogen forms for the highly productive wetland grass *Arundo donax*, a candidate species for wetland paludiculture. Ecological Engineering, 105, 379–386.

USDA Invasive Species. (n.d.). Retrieved from https://www.aphis.usda.gov/aphis/ourfocus/wildlifedamage/operational-activities/sa_invasive/ct_invasive_species1

Vogelmann, J. E., Rock, B. N., & Moss, D. M. (1993). Red edge spectral measurements from sugar maple leaves. *International Journal of Remote Sensing*, *14*(8), 1563–1575. https://doi.org/10.1080/01431169308953986

Xie, Y., Sha, Z., & Yu, M. (2008). Remote sensing imagery in vegetation mapping: a review. *Journal of Plant Ecology*, *1*(1), 9–23. https://doi.org/10.1093/jpe/rtm005